Available online at www.sciencedirect.com
SCIENCE DIRECT®

International Journal of Heat and Fluid Flow 26 (2005) 411–415

International Journal of HEAT AND FLUID FLOW
www.elsevier.com/locate/ijhff

Surface flow visualization using thermal tufts produced by an encapsulated phase change material

Jason S. Smith [a], James W. Baughn [a,*], Aaron R. Byerley [b]

[a] *Department of Mechanical and Aeronautical Engineering, University of California, Davis, CA 95616, USA*
[b] *Department of Aeronautics, US Air Force Academy, Colorado Springs, CO 80840, USA*

Accepted 7 October 2004
Available online 18 December 2004

Abstract

A new thermal tuft method for flow visualization similar to the laser thermal tuft method is described. The earlier laser thermal tuft method involved heating a spot on a surface with a laser, producing a teardrop temperature distribution on a surface coated with thermochromic liquid crystals. In the present study, thermal tufts are produced by embedding small thermal masses in a low thermal conductivity substrate. When a model is exposed to wind tunnel flow, the embedded thermal masses remain (nearly) isothermal while the thermal tufts appear downstream. The advantage of using embedded thermal masses over previous methods is that no laser or heated base is needed. Multiple tufts can easily be achieved. By using an encapsulated phase change material the phase change between solid and liquid (ice) produces isothermal spots. Images of the surface temperature distributions associated with these thermal tufts were obtained using both liquid crystal and infrared thermography. Flow visualization using these thermal tufts is demonstrated for an impinging jet and on a flat surface in a wind tunnel with crossflow.

Keywords: Tuft; Flow visualization; Phase change; Infrared; Liquid crystal; Thermal

1. Introduction and background

Surface flow visualization is useful for understanding flow in many applications and can be used to complement and validate computational studies of complex flow. A recent development in non-intrusive surface flow visualization is the "laser thermal tuft". (Baughn et al., 1995), first described this technique in a study to determine where flow separation had occurred on the suction side of a turbine blade. This technique was later patented by the USAF (River et al., 1999). The principle behind this method was to use a laser to heat a spot on a surface coated with microencapsulated thermochromic liquid crystals (TLCs). This circular heated laser spot (~3 mm) creates a distinct thermal pattern or tuft downstream by advection in the direction of surface airflow. The thermal tuft was a teardrop shape color change in the TLCs pointing in the downstream direction. Using this method, Baughn et al. (1995) were able to determine the location of boundary layer separation on a turbine blade model in a cascade wind tunnel. They pointed out that multiple spots could be obtained by using a Laser Tuft Matrix (LTM). In the location of boundary layer separation or reattachment, the thermal tuft is circular and centered around the laser spot with no hint of a teardrop shape. Further demonstrations of the laser thermal tuft were done by (Townsend, 1996). (Baughn et al., 1999), presented the results for a laser thermal tuft created by an infrared (IR) laser on the flow separation and reattachment on a turbine blade at low Reynolds numbers. The IR laser produced a clear red spot at the center of the thermal tuft. Their results are shown in Fig. 1.

* Corresponding author. Tel.: +1 719 333 9526.
E-mail addresses: jason.s.smith@lmco.com, james.baughn@usafa.af.mil (J.S. Smith).

0142-727X/$ - see front matter
doi:10.1016/j.ijheatfluidflow.2004.10.004

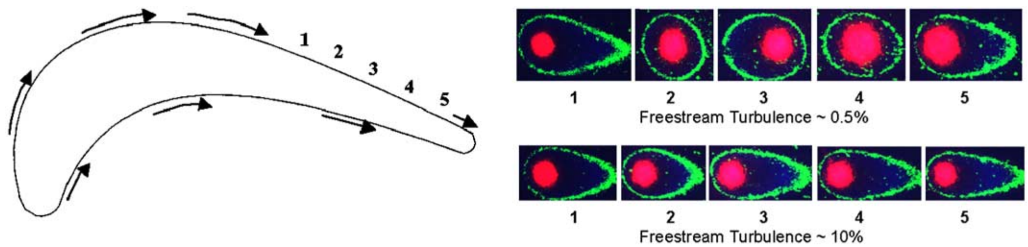

Fig. 1. Laser thermal tuft on a turbine blade (Baughn et al., 1999).

For their case where freestream turbulence was 0.5%, separation occurred at location 2, while reattachment occurred at location 4. Between location 2 and 4 was a region of recirculation, indicated by the tail of the thermal tuft pointing in the opposite direction of freestream at location 3. At high freestream turbulence, they were able to show that the flow remained attached; the laser tuft images all point in the direction of the freestream flow.

Further applications of the laser thermal tuft were done by (Butler et al., 2001), and (Byerley et al., 2003). These studies also used the laser thermal tuft to determine the location of flow separation and reattachment. In addition, (Byerley et al., 2003), introduced a dimensionless term to quantify the strength of the laser tuft called the eccentricity. Using a similar principle as the laser thermal tuft, (Batchelder and Moffat, 1998), described a surface flow visualization technique using heat sinks with "pin fins" to create an array of small hot spots on a surface.

A "cool" thermal tuft was produced by (Byerley et al., 2001), where IR heaters were used to uniformly heat a black surface with reflective spots affixed to the surface. The reflective surface remained cool while the surrounding surface heated up and produced a thermal tuft downstream of the "cool" spot.

The purpose of the present research was to develop a new thermal tuft method using an embedded thermal mass with an encapsulated phase change material. The capsules use the phase change between solid and liquid (ice in the present study) to produce isothermal spots. A matrix of embedded capsules is used, providing surface flow visualization at different locations on a model surface.

2. Principles of the thermal tufts

We define a thermal tuft here, in reference to surface flow visualization, as a teardrop shaped temperature pattern on a surface, originating from a heated or cooled spot, pointing in the direction of the surface flow. The thermal tuft is generated by advection causing the heated or cooled air to interact with the surface downstream of the thermal spot. The region surrounding the thermal tuft involves heat transfer in both convection and conduction.

For boundary layer flow, the characteristics of the boundary layer play an important role in the shape and size of the thermal tuft. The two types of boundary layers affecting the thermal tuft are the velocity boundary layer and thermal boundary layer. The hydrodynamic- or velocity boundary layer begins upstream of the thermal tuft. The thermal boundary layer begins at the heated or cooled spot and dissipates downstream of the spot, creating the thermal tuft. It is thin compared to the velocity boundary layer. The size of the heated or cooled spot is small with respect to the change in thickness of the velocity boundary layer over the distance of the spot which means that the velocity profiles at the beginning and at the end of the spot remain relatively unchanged. The shape of the thermal tuft is determined by the dissipation of the thermal boundary layer and the heat transfer to the substrate.

3. Encapsulated phase change material—model design

The materials used in the model and base must have a low thermal conductivity in order to produce a clear thermal tuft. An advantage of having a base material with low thermal conductivity is the short thermal time constant. After some analysis, polystyrene foam was selected as the base material for the present study. In order to have a smooth surface, a layer of foam filled poster board was used. It was painted with black matte finish paint then airbrushed with TLCs. The model consisted of a 3×3 matrix of capsules spaced 2.5 cm apart. This model was designed to plug into a base producing a flat plate that would be mounted in a wind tunnel. A diagram of the encapsulated phase change capsule is shown in Fig. 2.

The capsules were made from copper tubing with brass end plugs. The brass plug on the top surface of the tuft was soldered into place and machined flat to maintain a smooth model surface. A small piece of polystyrene foam was inserted into the capsule to compensate for the expansion of ice during the freezing process. The bottom of the capsules was sealed with another brass plug using epoxy cement.

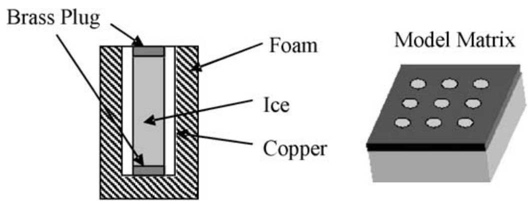

Fig. 2. Diagram of encapsulated phase change material and model matrix.

4. Experimental setup and procedure

Measurements were made on a flat plate in an open environment using an impinging jet and in a wind tunnel with crossflow. For the impinging jet measurements a Badger airbrush (also used to spray the models with a coating of TLCs) was positioned 9.5 cm above and normal to the model surface at the corner of the matrix above one of the capsules. For the wind tunnel measurements, the capsules were embedded in a flat plate that was mounted in the freesteam flow of a 30.5 cm × 30.5 cm wind tunnel. The experimental procedure begins when the models are removed from a freezer at approximately −6 °C and placed under the impinging jet or in the wind tunnel.

Approximately 2 min after being removed from the freezer, the capsules reached a phase change equilibrium and remain isothermal for several minutes during the measurements. During this isothermal period the capsules are at 0 °C.

5. Liquid crystal measurements/sony camera

For the liquid crystal measurements we chose a moderate band TLC (R12C6W). A 5 mega-pixel Sony DSC-F717 digital camera (5× optical zoom) was used to capture the images of the thermal tufts. The RGB images were captured in both jpeg and tiff format with a resolution of 2560 × 1920 pixels.

6. Infrared thermography

Using IR thermography to detect the thermal tufts is an alternate approach to the use of liquid crystal thermography. The thermal resolution for IR cameras is given in terms of the noise equivalent temperature difference (NETD) or the temperature difference that two black body radiators need in order to produce a difference in the camera signal equal to signal noise. Lower-end IR cameras have a NETD on the order of 0.12 °C while higher end cameras have a NETD as small as 0.02 °C. The IR camera used here was a Mitsubishi IR-M700 with a NETD of 0.08 °C. It had a resolution of 801 × 512 pixels and operated in the 3–5 μm range. A ruby–sapphire window was used which was rated for transmission up to 5 μm.

7. Results and discussion

7.1. Thermal tufts—using TLCs

The thermal tufts and flow visualization for the impinging jet are shown in Fig. 3(a). The jet was directed at the upper left hand capsule. The resulting flow field clearly shows the flow spreading out from the impingement point of the jet and illustrates that this method can easily be used for multiple surface flow measurements. The thermal tufts closest to the impinging jet are smaller, possibly due to a larger freestream velocity and shear stress. The thermal tufts further away are larger, possibly due to a smaller freestream velocity and corresponding shear stress. A stagnation point was observed at the capsule directly below the impinging jet.

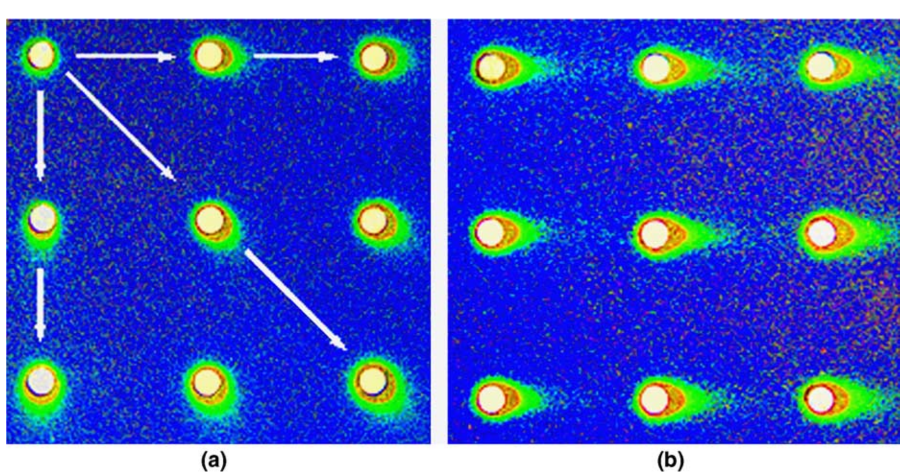

Fig. 3. Hue images of EPCM thermal tufts (a) impinging jet, and (b) crossflow at 5 m/s.

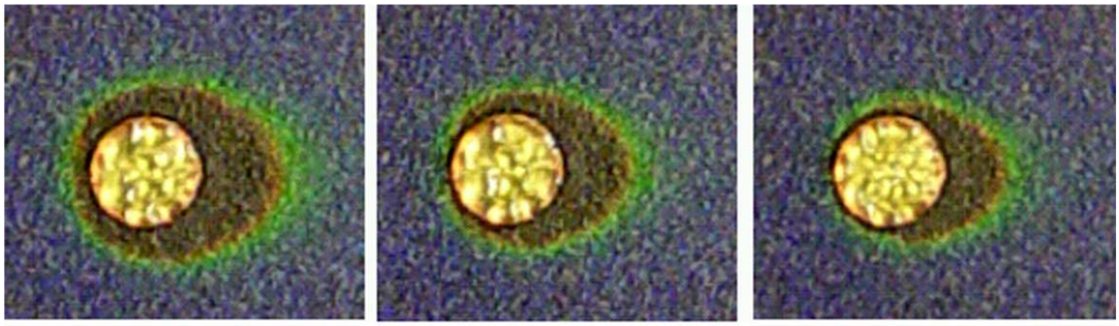

Fig. 4. RGB images of thermal tufts at three different freestream velocities.

The thermal tufts and flow visualization in the wind tunnel with crossflow are shown in Fig. 3(b). The teardrop shape, indicating the airflow moving from left to right in a uniform manner is clearly shown. The performance of the thermal tufts at three different freestream velocities was studied: the RGB images at 5 m/s, 10 m/s and 20 m/s for one capsule are shown in Fig. 4.

The thermal tufts in Fig. 4 are all located in the center of the matrix of Fig. 3(b) at a distance of 28 cm from the leading edge of the flat plate. This sequence of images shows the tuft length decreasing as freestream velocity and Reynolds number increases. The thermal tufts at 5 m/s have the longest tail and width (dimension perpendicular to the airflow). As velocity increases to 10 m/s, the tail shortens along with the width. Similarly, when velocity is increased to 20 m/s, the tail shortens further and the width decreases further. The local Reynolds numbers for these tufts ranged from 48 000 to 192 000. Boundary layer measurements suggested a turbulent boundary layer (apparently tripped by the sharp leading edge).

One issue that arose with the use of ice in the capsules was condensation on the tuft surface, which can be slightly seen on the copper/brass portion of the tuft in Fig. 4. Condensation occurs because the capsule surface was below the dew point temperature. In later runs, the amount of time between removing the model from the freezer and beginning the experiment was reduced in order to decrease the condensation. Condensation did not appear to occur in the wind tunnel flow.

7.2. Thermal tufts—using IR thermography

The IR camera was used to capture images simultaneously with the Sony digital camera. The surface of the model was at approximately 20 °C while the thermal tuft surface was near 0 °C. The temperature difference of 20 °C was split into 256 values. This meant that each pixel could display temperature to the nearest 0.08 °C, ranging from 0 °C at the capsule surface to 20 °C on the surrounding surface.

An enhanced image was created by applying a gradient map using Adobe Photoshop as shown in Fig. 5.

The color scheme used in Fig. 5 [1] was selected to roughly simulate the TLC color play. The gradient map in the Figure shows the colors assigned to each grayscale pixel. A disadvantage to the IR image was that the circular spot outline was not as distinct as the RGB images in Fig. 4. Some minor image editing was performed in Fig. 5 in order to re-define the circular spot outline. The emissive properties of the capsule surface are low in comparison to the black model surface (Polished brass has an emissivity of about 0.1 while the flat black paint has an emissivity of about 0.94). This difference in emissivity and perhaps condensation may have altered the image, slightly distorting the true circular spot.

The thermal tufts obtained using IR imaging are quite similar to those using liquid crystal thermography, and provide comparable flow visualization. The advantage of using IR imaging is that it is not necessary to spray the model with TLCs, nor to be concerned with the choice of temperature and bandwidth for the TLCs. The disadvantage is the cost of the IR camera and the need for an expensive window in the wind tunnel that transmits in the IR range.

7.3. Effect of reynolds number, shear stress and velocity

Since the thermal boundary layer associated with the thermal tufts is thin compared to the hydrodynamic boundary layer, it is suspected that the tuft length and shape depends on velocity profile near the wall and thus the wall shear stress. If so, the thermal tufts could possibly be used for measuring wall shear stress. Measurements were attempted in the wind tunnel to determine whether the shape or length of the thermal tufts investigated here could be correlated with shear stress and or

[1] For interpretation of color in Figs. 1, 3, 4 and 5, the reader is referred to the web version of this article.

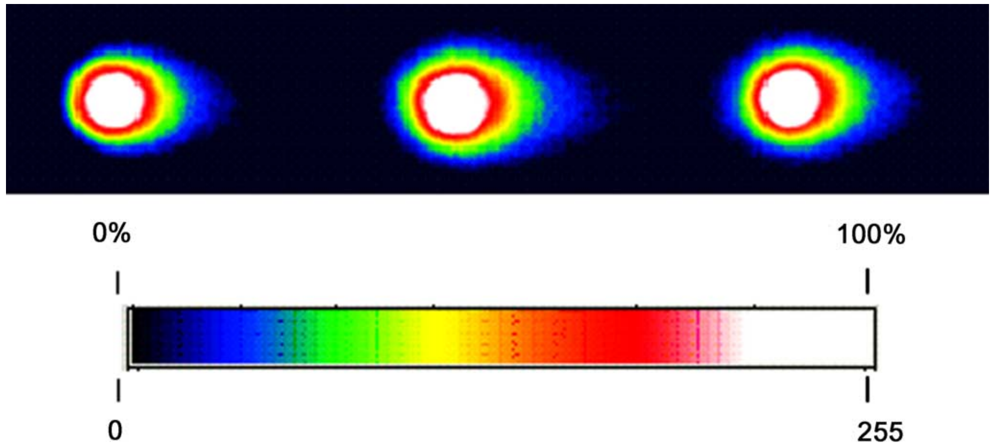

Fig. 5. Enhanced IR image of the EPCM thermal tufts.

velocity. Unfortunately, the boundary layer appeared to transition early and no direct correlation with shear stress or other flow parameters was possible. It was observed that the thermal tufts here increased in length with distance from the impinging jet (lower velocity and shear stress) and also increased in length with decreasing velocity in the wind tunnel. It was concluded that the size and shape of the thermal tuft does depend on the boundary layer thickness and profile and thus possibly the wall shear stress. The exact cause for the variation in size of these thermal tufts is not yet established and is being investigated.

8. Summary and conclusions

The use of an encapsulated phase change material (ice) can produce clear thermal tufts. These tufts were captured using liquid crystal thermography which provided clear RGB and hue images of the thermal tufts. They were also captured using an IR camera. Flow field visualization using this new method was illustrated for an impinging jet and for a flat plate in cross flow.

Using ice as the phase change material proved to be a convenient and simple method of creating an isothermal capsule for the thermal tufts. Other phase change materials were considered such as Cesium, Potassium, Calcium Chloride, Glycerin, and wax. Several of these were tested. Calcium Chloride and Glycerin did not provide a clear phase change temperature. Wax showed a narrow enough temperature region for the phase change that clear thermal tufts were obtained. Other phase change materials may be suitable and could be investigated if it is desired to use a heated (instead of a cooled) model to produce the thermal tufts.

Further investigation of the effect of Reynolds number, velocity, and wall shear stress on thermal tuft length and shape is needed and is currently being investigated.

References

Batchelder, K.A., Moffat, R.J., 1998. Surface flow visualization using the thermal wakes of small heated spots. Exp. in Fluids 25, 104–107.

Baughn, J.W., Butler, R.J., Byerley, A.R., River, R.B., 1995. An experimental investigation of heat transfer, transition and separation on turbine blades at low reynolds number and high turbulence intensity, ASME Paper No. 95-WA/HT-25. In: Proc. 1995 Int. Mech. Eng. Congr. Expositions, San Francisco, CA, USA.

Baughn, J.W., Mayhew, J.E., Butler, R.J., Byerley, A.R., Rivir, R.B., 1999. Turbine blade flow separation and reattachment at low reynolds numbers. J. Heat Transfer, 121, August Insert.

Butler, R.J., Byerley, A.R., Van Treuren, K., Baughn, J.W., 2001. The effect of turbulence intensity and length scale on low-pressure turbine blade aerodynamics. Int. J. Heat Fluid Flow 22, 123–133.

Byerley, A.R., Stormer, O., Baughn, J.W., Simon, T.W., Van Treuren, K.W., List, J., 2003. Using gurney flaps to control laminar separation on linear cascade blades. J. Turbomachinery 125 (1), 114–120.

Byerley, A.R., Stormer, O., Baughn, J.W., Simon, T.W., Van Treuren, K.W., 2001. A cool thermal tuft for detecting surface flow direction. J. Heat Transfer 124, 594.

River, R.B., Baughn, J.W., Townsend, J.L., Butler, R.J., Byerley, A.R., 1999. Thermal tuft fluid flow investigation apparatus with a color alterable thermally responsive liquid crystal layer. United States patent no. 5963292.

Townsend, J.L., 1996. A laser thermal tuft using liquid crystals for flow visualization, M.S. Thesis, University of California, Davis.